

RESONANCES INFLUENCE IN RECESSED-MOUNTED TRANSDUCERS USED FOR UNSTEADY PRESSURE MEASUREMENTS

Antonio Sanz Luengo

Royal Institute of Technology
Chair of Heat and Power Technology
S-100 44 Stockholm, Sweden
ansl@kth.se

Damian M. Vogt

Royal Institute of Technology
Chair of Heat and Power Technology
S-100 44 Stockholm, Sweden
damian.vogt@energy.kth.se

Torsten H. Fransson

Royal Institute of Technology
Chair of Heat and Power Technology
S-100 44 Stockholm, Sweden
torsten.fransson@energy.kth.se

ABSTRACT

The present paper analyzes the influence of resonances in recessed mounted transducers for measuring unsteady pressures in turbomachinery related test facilities. Due to the difficulties of the unsteady measurements in this kind of setups, recessed mounted technique allows increasing the resolution of measurement points, transducer exchangeability, fair operation conditions, and cost reduction with respect to other procedures. However the intrinsic nature of this procedure requires a duct which connects the control volume to be measured and the transducer, producing damping and phase lagging of the signal due to the pipe. In consequence a dynamic calibration is required for being able to evaluate these effects through a transfer function. This dynamic calibration can show up the presence of resonances due to the duct properties. These resonances are studied in this paper for determining its influence on the measuring capabilities, as well as an overview of the different tuning capabilities at the interest frequency bands.

NOMENCLATURE

f	frequency
D	dynamic calibration damping
P	pressure
\hat{P}	unsteady pressure (complex)
t	time
V	voltage
δ	infinitesimal increment
Δ	associated uncertainty
φ	signal phase
\emptyset	dynamic calibration phase lag

Subscripts and Superscripts

n	specific frequency
pos	related to the positioning error
ref	related to the reference transducer
stc	related to the stochastic error
std	steady
sys	related to the systematic error
td	related to the recessed mounted transducer

Abbreviations

FFT fast fourier transformation

INTRODUCTION

In turbomachinery aeromechanics, the correct measurement techniques and measurement uncertainties are of crucial importance for the correct understanding of unsteady aerodynamic interactions. Among these phenomena the aerolastic interactions show up as the most challenging from the experimental point of view due to the complex working conditions. Flutter is one of this phenomena, it is produced by a structural, fluid dynamic interaction which generates a self-excited and self-sustained instability. This can lead to high vibration amplitudes, producing ultimately, machine failure due to high cycle fatigue. The instability is generated due to the unsteady pressures applied on the blade surface, interacting with the blade movement. This fact makes this unsteady pressure the fundamental objective of the measurements.

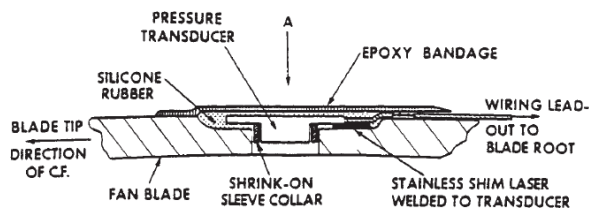


Figure 1 Embedded Transducer assembly

The interaction of the structural and fluid dynamics implies that the instrumentation should not interfere both in the fluid and in the blade structure. Normally the instrumentation is mounted inside the blade modifying the structural performance, in addition the evolution of turbomachines lead to more slender blades with high 3D shapes. This fact complicates the instrumentation and shows up the needing off less invasive procedures.

Furthermore flutter is a phenomenon extremely sensible to unsteady pressures, in consequence the measurements require highly time-accuracy which implies fast response transducers and high sensitivity due to the low pressures that can initiate the self-excitation.

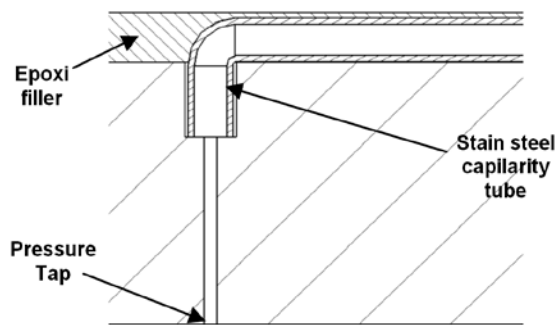


Figure 2 Recessed mounted pressure tap

Traditionally these measurements have been done using embedded miniature transducers (Figure 1), which provides a direct pressure measurement. This kind of assembly provides very good results while properly calibrated for the working conditions but with high limitations regarding cost, physical embedding, measuring resolution, inertial effects, thermic effects, and other operating problems produced by the structure-transducer interaction.

As an alternative recessed-mounted transducers consist on the assembly of the transducer outside the test object, linking it with the flow domain using capillary tubes between 50mm and 150mm (Figure 2).

This procedure presents some interesting advantages with respect to the traditional one. It is cheaper because of the inter exchangeability of the transducers, and in consequence de reduction on the transducer number. It allows detailed measurement resolution, the instrumentation can be highly noninvasive but depending on the number of measuring points. On the other hand, the duct properties produce signal attenuation and a phase lagging of the signal, which implies a bigger postprocessing of the data.

For being able to obtain an accurate measurement it is necessary to calibrate dynamically the complete setup. The dynamic calibration analyzes the behavior of the system regarding amplitude and phase of the complex pressure at different frequencies. This procedure is done using an in-house calibrating procedure which compares the response obtained by a pressure pulse train on a reference transducer (direct measurement), and on the recessed-mounted one. With this information is possible to generate a transfer function that corrects the response of the transducer with reality.

The present study shows up the presence of system resonances and analyzes the possible consequences along the processing system regarding uncertainty.

CALIBRATION SET UP

The calibration system is composed of 3 different parts:

- Pressure pulse generator
- Calibration probe (miniature reference cavity)
- High-speed data acquisition system.

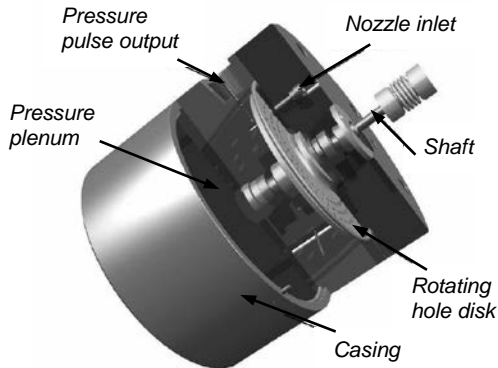


Figure 3 Pressure pulse generator set up

The pressure pulse generator is siren type, consisting on a miniaturized nozzle that generates a fluid jet (air) which collides with a three row hole perforated disk. This disk is driven by a speed controlled DC motor so setting a determined rotational speed of the disk will interfere the pressure jet a number of holes times the rotational frequency. The presence of 3 hole rows on the rotating disk produces the presence of different harmonics into the pressure signal but with dominating influence of the first harmonic which will be the one used for the dynamic calibration. The pressure pulse is driven outside through an output tube collinear with the nozzle that connects with the calibration probe. The disk is isolated in a pressure chamber connected to a pressure plenum. Modifying the plenum pressure the disk gets pressurized and in consequence output mean pressure intensity level can be set. The relation between the nozzle inlet pressure and the plenum pressure will define the intensity of the unsteady pulse generated.

The reference cavity consist on a cylindrical control volume (1.8mm \varnothing x 3mm h) with a reference fast response piezoelectric pressure transducer (Kulite XCQ-062, 1.6bar abs) on one extreme of the volume, the pressure tap to calibrate is set on the other extreme of the cavity being the cavity sealed with an O-ring. The pressure pulse is transferred from the pressure pulse generator with a capillarity tube. The pulse enters through a side hole in the mid-section of the cavity. For being able to ensure the flow channel symmetry, in the opposite position, an outlet tube has been introduced, connected to a long capillarity tube which ensures no reflections. In this way the reference cavity is completely symmetric defined, and the wave symmetry is guarantee.

The pressure taps to calibrate are connected with capillarity tubes to the recessed mounted transducers (Kulite XCQ-062, 1.6bar abs). These transducers are statically calibrated using a Druck DPI-603 (100Pa accuracy) to minimize uncertainties. The high-speed data acquisition is done with the system Kayser-Threde KT8000, which also provides a stabilized sensor excitation (10VDC). The system provides 32 channels with programmable amplifiers and 14bit A/D conversion for a maximum sampling rate of 200kHz.

The system featured 32 channels with programmable amplifiers, 14bit A/D conversion for each channel and a maximum sampling rate for all 32 channels simultaneously of 200kHz. Each channel could be programmed individually such as to set gain and a low-pass filter with variable cut-off frequency. The present tests were performed with a gain of 10, no low-pass filtering and at a sampling rate of 20kHz.

The standard calibration procedure consists of 3 steps:

- Reference cavity positioning and centering
- Data acquisition (KT8000)
- Postprocessing. Frequency spectrum, signal attenuation, phases lagging, transfer function acquisition.

TEST OBJECT (Baseline configuration)

The blade used in this experiment is a low pressure turbine with a high lift profile. The test tap was situated in the suction side at 90% of the span. The instrumentation has been done using a stainless-steel tube of 0.5mm of internal diameter embedded on a groove that communicates the tap with the root of the blade. The pressure tap of 0.4mm diameter is perpendicular to the surface, the connection with the stainless-steel pipe can be done in many different ways but the most interesting for our case due to the simplicity and the leak-free robustness is the procedure shown in

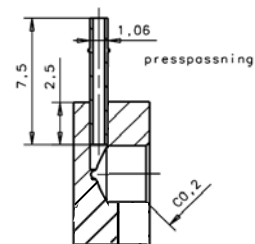


Figure 4 Transducer housing

Figure 2. This procedure uses an L-bended pipe that smoothly conduits the pressure signals. The length of the pipe from tap to root is 150mm.

The blade is connected to the transducers housing through a vinyl pipe (50mm), a fast connector and another vinyl pipe (25mm). The first vinyl pipe length and shape will be studied later as a possible way of modifying the response of the overall system response.

The fast response transducers are accommodated on a brass housing (Figure 4). This housing consists on a signal intake that communicates the cavity, where the transducer membrane lies, with the tap pipe line.

RESONANCE INFLUENCE, UNCERTAINTY ASSESSMENT

For analyzing the influence of the resonance influence on the system it has been necessary to set up an uncertainty model of the system. This model, is divided principally between the errors due to calibration and the raw measurement own errors.

RAW Measurement Uncertainty

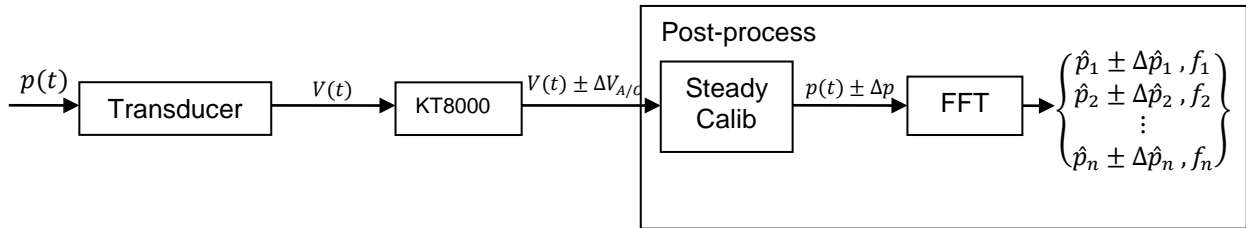


Figure 5 Pressure measurement diagram. Uncertainty propagation

As shown in Figure 5, the fast response transducer transforms the pressure into a voltage in the time domain the error introduced in the measurement by the transducer is not considered stochastic, which implies that the possible offset remains constant for all the measurement along the time and in conclusion can be neglected while analyzing the unsteady part. Due to the amplification of the signal and the A/D converter, the high-speed acquisition system (KT8000) introduces a new error in the measurement. This error depends on the gain set. For the present paper all the analysis has been done with the calibration settings determined in Table 1.

Table 1

Unsteady Intrinsic System error		
A/D converter(100mV, gain=10)	$\pm \Delta V_{A/D}$	$\pm 6.1 \mu V$
TD sensibility(Pa)	$\pm \Delta p_{TD}$	$\pm 10 Pa$

For translating the electric signal into pressure, the voltage is multiplied by the steady calibration parameter. The pressure error is obtained applying the “root-sum-square error linear approximation” [x]

$$p = k_{td \text{ std calib}} \cdot V \tag{Eq. 1}$$

$$\Delta p = \sqrt{\left(\frac{\partial p}{\partial k} * \delta k\right)^2 + \left(\frac{\partial p}{\partial V} * \delta V\right)^2} + \Delta p_{TD} = \sqrt{(V * \Delta k)^2 + (k * \Delta V)^2} + \Delta p_{TD} \tag{Eq. 2}$$

Due to the nature of the steady calibration the deviation transformation will produce an offset in the calibration curve not modifying its slope, as the objective is the analysis of the unsteady behavior, the $k_{td \text{ std calib}}$ error can be depreciate, being the error reduced to the equation x.

$$\Delta p = k_{td \text{ std calib}} * \Delta V + \Delta p_{TD} = 1698.7882 \frac{kPa}{V} \cdot \pm 6.1 \mu V + \pm 10 Pa = \pm 20.3626 Pa \tag{Eq. 3}$$

The pressure signal is transformed into the frequency domain using a FFT (Fast Fourier Transformation). For avoiding signal truncation problems, a preliminary FFT has been applied on the original signal with the

frequency obtained it has been defined the period of the signal, and the signal has been delimited by a multiple of the period. At this point is very important to keep in mind that the error associated with the pressure measurement not only depends on its absolute value but on the distribution pattern along the signal. This means that for a sinusoidal signal with a frequency f the most prejudicial error pattern corresponds to an error signal with the same frequency. While translating to the frequency domain the signal error will be decomposed into a modulus error and phase error.

For calculating the error progression along the FFT the time-domain pressure has been perturbed with an error signal with the error amplitude and the main harmonics of the original signal. These 2 elements can be expressed as phasors, Figure 6

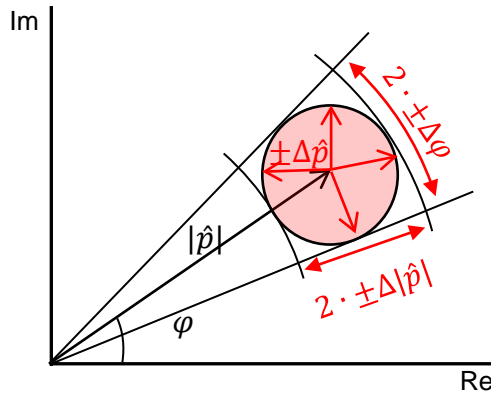


Figure 6 Complex pressure uncertainty propagation scheme

The uncertainty subjected to an unsteady pressure measurement using the described set up, reveals that the modulus uncertainty remains constant and only depends on the transducer characteristics. The phase uncertainty depends both on the intrinsic characteristics of the transducer but also on the pressure measured as shown in Figure 6. This implies that the bigger the measurement amplitude the smaller the phase error.

Calibration Uncertainty

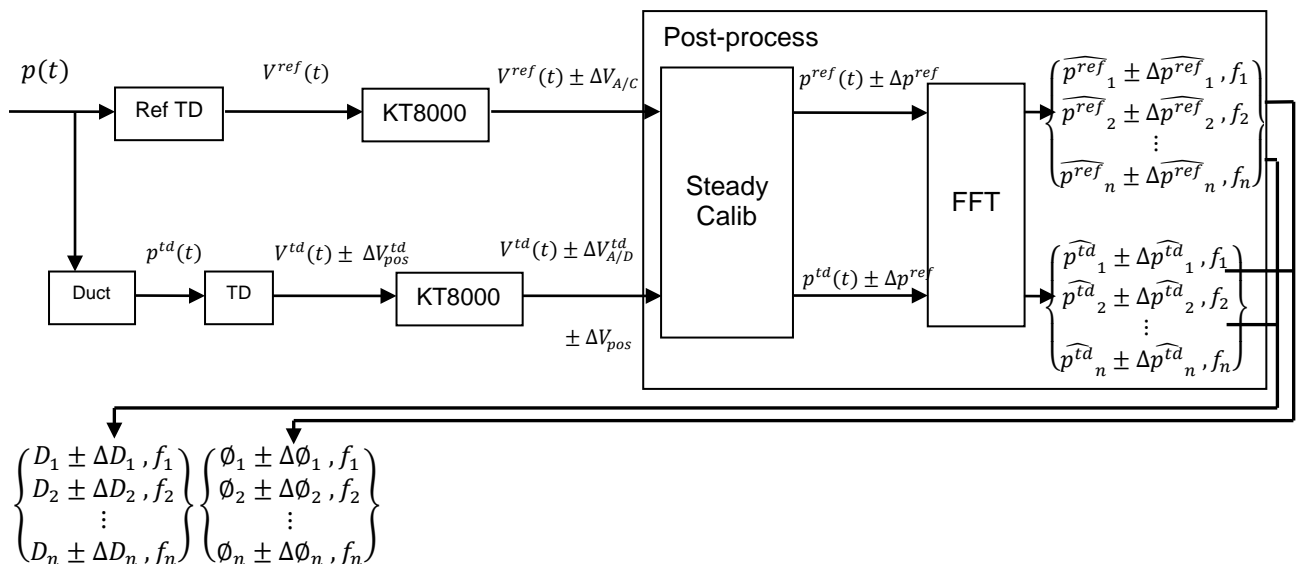


Figure 7 Calibration process diagram. Uncertainty propagation

The calibration procedure can be modeled as shown in Figure 7. The pressure signal $p(t)$ generated by the pressure pulse generator reach the reference cavity where is captured by the reference transducer. The same pulse is communicated to the pressure tap, and depending on the position of this tap with respect to the reference cavity a positioning uncertainty is introduced. The pulse travel along the duct to the transducer connected to the piping modifying in the way its characteristics. Both transducers transform the pressure into an analogic electric signal within the transducer sensibility. In the high speed acquisition module the analog signal is amplified and transformed into a digital signal, this introduces another uncertainty source.

Both signals are post-processed and correct with the steady calibration and transformed into the frequency domain, where the damping coefficient and phase lag values are determined for each frequency, allowing to estimate the reference signal with the one measured in the tap transducer.

The calibration procedure uncertainty analysis has been done from 2 different perspectives, from the theoretical point of view using 2 raw pressure measurement uncertainty progression lines that end with the determination of the signal damping and lagging. Form the statistical point of view for determining the influences of other parameters on the overall uncertainty, as for example the error in the probe positioning or the random error inherent to the system. There are other possible sources of error that have not been included as the sampling frequency error, this will be studied in future experiments.

The error of the vectors D and \emptyset can be decomposed into a systematic error of the procedure itself, an stochastic error of unknown source, and a positioning error depending on the position of the reference cavity with respect to the tap .

$$\Delta D = \Delta D_{sys} + \Delta D_{stxc} + \Delta D_{pos} \quad \text{Eq.4}$$

For determining these errors different methods have been used:

-The calibration systematic error, assumed as the error inherent to the system accuracy, has been determined through the “root-sum-square error linear approximation”.

$$D_n = \frac{|p_n^{td}|}{|p_n^{ref}|} \quad \text{Eq.5}$$

$$\Delta D_n = \sqrt{\left(\frac{\partial D_n}{\partial |p_n^{td}|} * \delta |p_n^{td}| \right)^2 + \left(\frac{\partial D_n}{\partial |p_n^{ref}|} * \delta |p_n^{ref}| \right)^2} = \sqrt{\left(\frac{1}{|p_n^{ref}|} * \Delta |p_n^{td}| \right)^2 + \left(\frac{|p_n^{td}|}{|p_n^{ref}|^2} * \Delta |p_n^{ref}| \right)^2} \quad \text{Eq.6}$$

$$\emptyset_n = \varphi_n^{ref} - \varphi_n^{td} \quad \text{Eq.7}$$

$$\Delta \emptyset_n = \sqrt{\left(\frac{\partial \emptyset_n}{\partial \varphi_n^{ref}} * \delta \varphi_n^{ref} \right)^2 + \left(\frac{\partial \emptyset_n}{\partial \varphi_n^{td}} * \delta \varphi_n^{td} \right)^2} = \sqrt{\Delta \varphi_n^{ref}^2 + \Delta \varphi_n^{td}^2} \quad \text{Eq.8}$$

-The positioning error has been determined, experimentally. The probe has been positioned in 6 different positions 2 centered and 4 eccentric and equally spaced around the reference cavity. As the set-up is identical for each position, it can be assumed that the stochastic error and the systematic as identical, so the positioning error can be estimated as the standard deviation of the experiments set.

-The sampling error has been determined with the same procedure as the one used for the positioning error. 6 different sampling frequencies have been used for estimating this error. As indicated before the truncation of the signal has been prevented, for avoiding possible disturbances. (Figure 8 blue dots)

-The Stochastic error has been determined with the following criteria. 20 different measurements have been done, with exactly the same set up, same probe position, same sampling frequency, and in the same

measurement campaign. Under this conditions it is assumed that the standard deviation of the experiment test correspond to the stochastic error. (Figure 8 red dots).

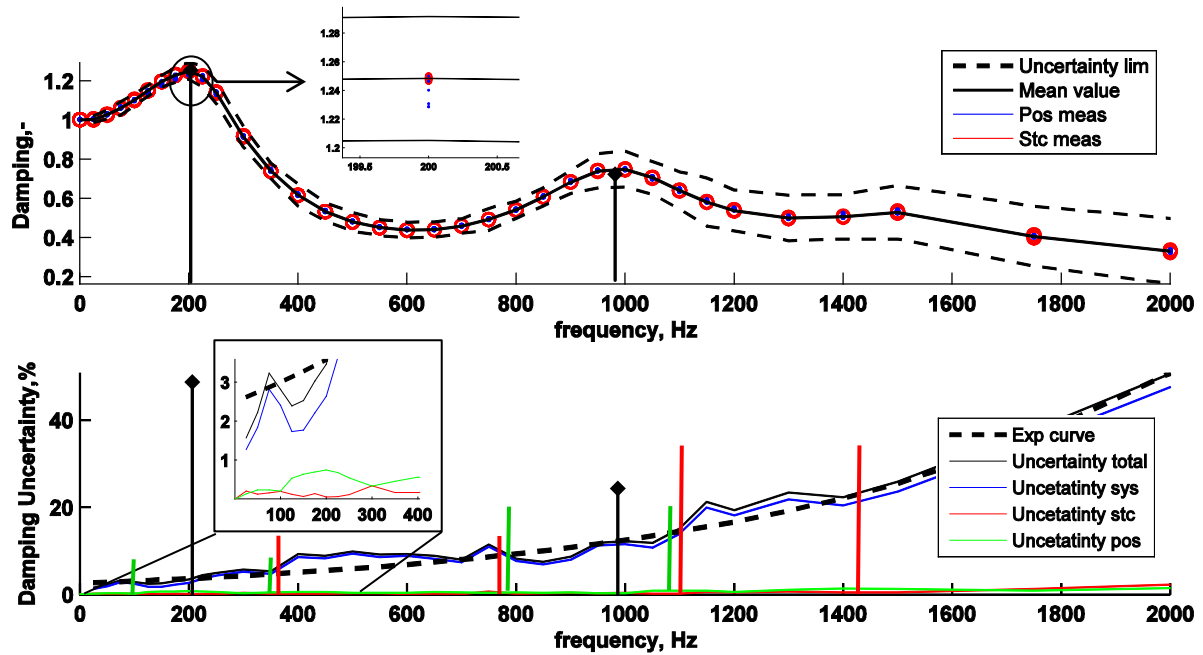


Figure 8 Damping and Damping uncertainty. Calibration diagram

With the data obtained in the experiments, the transducer-duct, damping and phase lag characteristic curves have been obtained, up to a frequency of 2000Hz that is very far away of the interest band that goes from 0 to 300Hz. The reason is to obtain a wide perspective of the behavior along the frequency band.

In the studied band 3 resonances have appeared being the first harmonic directly in the area of interest (Figure 8 up). The calculated uncertainty lies down a 6% for the band of interest. Is also observed that the dispersion of the data apparently is very small which indicates a priori that the determination of the damping is very stable. The uncertainty of the measurement has been introduced with the dashed lines in Figure 8 up.

Analyzing the influence of the each source of error it is evident that the bigger uncertainty source is the theoretical systematic error with respect to the positioning and random experimental uncertainties. Analyzing the overall uncertainty of the damping, an exponential uncertainty increase with the frequency (dashed line Figure 8 down) has been assumed. On this curve it can be appreciated that the overall uncertainty it is not spoiled due to the resonance peaks. Focusing on the 200Hz and 800Hz surroundings the uncertainty is increased with respect to the exponential while decreasing the resonance effect (400-800Hz). The uncertainty decreases again while starting the second resonance and quickly increased while its effect is minored (1100-1400Hz)

The influence of the resonance onto the damping is a high nonlinear process. If the resonance presence tends to reduce form a general point of view the uncertainty, it affects in a different way to the different error sources. In Figure 8 can be observed how the system uncertainty tends to be reduced with the resonances. Apparently a bigger damping should affect negatively the uncertainty according to the Eq.6 , but the percentual uncertainty shows a bigger amplification of the signal than the amplification of the uncertainty. The systematic uncertainty is subjected to the data acquisition system, and directly dependent on the reference and transducer modulus of the unsteady pressure and its associated error. Therefore for transducer and reference constant associated errors, the uncertainty tends to be reduced while increasing the unsteady pressures.

On another hand the positioning errors are increased around the resonances. The origin of this effect lies in the fact that the geometrical properties of the reference cavity are slightly modified. This necessary affects the tuning of the system varying the position of the resonance. This induces an uncertainty increase around these points.

In the end the random uncertainty does not seem to be significantly influenced by the resonances.

For the phase lag between signals a similar behavior is observed. But it is interesting to remark that the presence of a resonance increase the phase lag slope.

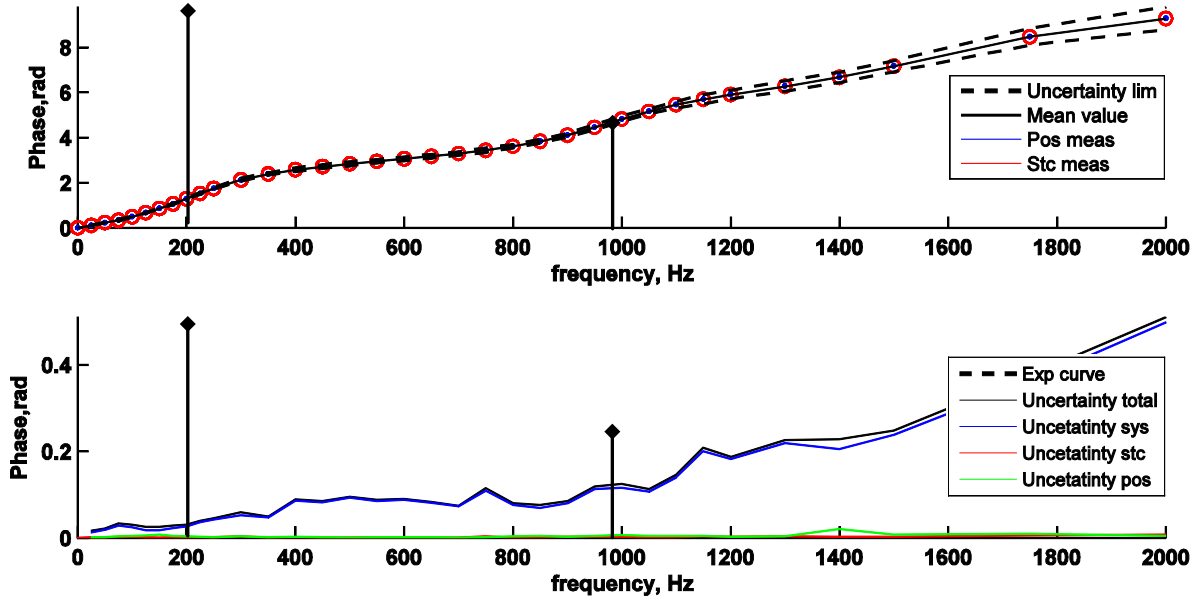


Figure 9 Phase lag and Phase lag uncertainty. Calibration diagram

For the set up used the main uncertainty source corresponds to the systematic one due to the range of measurements which defines the gain of the amplifier, the transducers... etc. The importance of the different uncertainty sources will change depending on the set up.

The pressure measured by the transducer is decomposed in its main frequencies modulus and phase. This pressure measurement is corrected with the damping and phase lag (equations XX and XX) and recomposed back for obtaining the estimation of the real unsteady pressure in the pressure tap inlet. The damping and phase lag deviation will be defined by the contribution of each uncertainty source taken into account, systematic, stochastic and position.

The uncertainty of the measurement is ultimately determined by the “root-sum-square error linear approximation” of the correction procedure shown below (Eq.9 and Eq.11).

$$|\hat{p}_n| = \frac{|p_n^{td}|}{D_n} \quad \text{Eq.9}$$

$$\Delta|\hat{p}_n| = \sqrt{\left(\frac{\partial|\hat{p}_n|}{\partial|p_n^{td}|} * \delta|p_n^{td}| \right)^2 + \left(\frac{\partial|\hat{p}_n|}{\partial D_n} * \delta D_n \right)^2} = \sqrt{\left(\frac{1}{D_n} * \Delta|p_n^{td}| \right)^2 + \left(\frac{|p_n^{td}|}{D_n^2} * \Delta D_n \right)^2} \quad \text{Eq.10}$$

$$\varphi_n = \varphi_n^{td} + \varphi_n \quad \text{Eq.11}$$

$$\Delta\varphi_n = \sqrt{\left(\frac{\partial\varphi_n}{\partial\varphi_n^{td}} * \delta\varphi_n^{td} \right)^2 + \left(\frac{\partial\varphi_n}{\partial\varphi_n} * \delta\varphi_n \right)^2} = \sqrt{\Delta\varphi_n^{td^2} + \Delta\varphi_n^2} \quad \text{Eq.12}$$

The result of this procedure is shown in Figure10. The overall uncertainty of the unsteady pressure modulus has an increase in general maintaining the shape of the damping uncertainty trend. Analyzing how each source

of uncertainty contributes to the overall uncertainty, $\Delta|p_n^{td}|$ seems to be the dominating factor which induces the uncertainty increase.

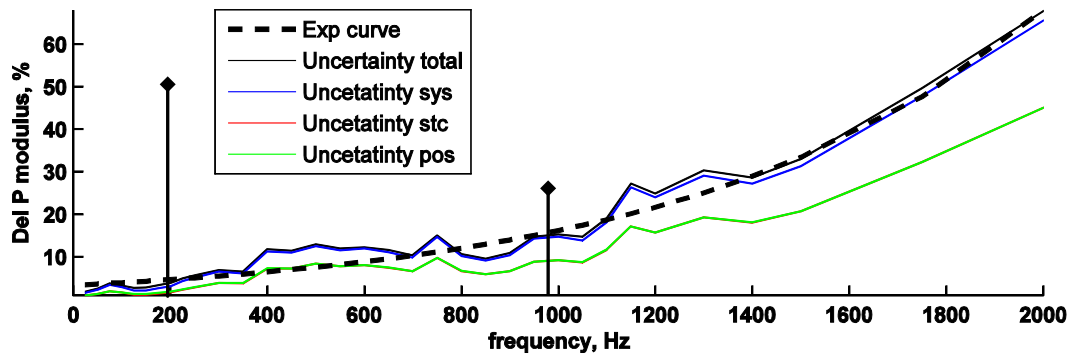


Figure 10 Unsteady pressure uncertainty graph

On the unsteady pressure phase uncertainty point of view as happened before with the modulus keeps the same trend of the phase lag but with an increase in the slope. The mayor contribution to the uncertainty is the one introduced by the transducer φ_n^{td} .

FLUTTER TEST SIGNAL RECONSTRUCTION, AND PROCEDURE IMPLICATIONS

At this point is interesting to have a clear perspective of the usage of this procedure. This system is used for measuring the unsteady pressures on the blade surface due to a controlled oscillation. With this set up a controlled flutter is modeled in the influence coefficient domain, measuring the unsteady pressures produced by the oscillation of one blade on itself and on the adjacent blades. From this point of view the analysis of the measurement uncertainty becomes complex due to the fact that for each frequency there is a modulus and phase measurement uncertainty. While reconstructing the wave depending on the number of harmonics used the uncertainty will change. The more harmonics involved the bigger the uncertainty associated with the estimated unsteady pressure.

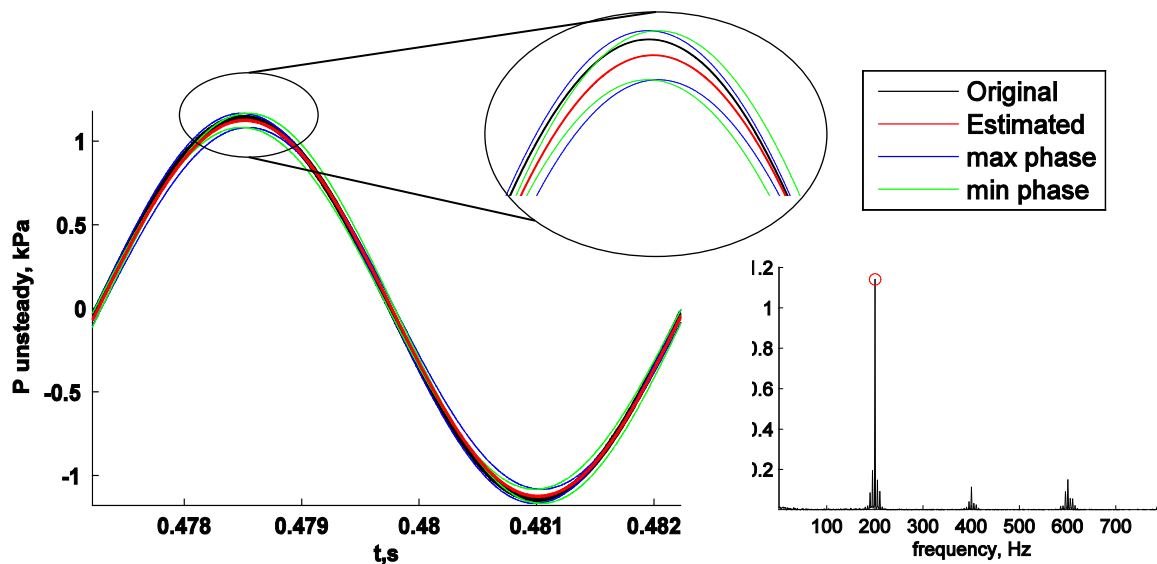


Figure 11 1st Harmonic reconstruction

For this specific case the blade is moved by a mechanical device which provides a harmonic motion at specific frequency (From 0 to 260Hz). It can be assumed that the mayor influence on the blade unsteady pressure will be produced by the motion frequency. This implies that analyzing the main harmonic of the unsteady pressure (that corresponds to the motion frequency), will provide a good approximation of the unsteady performance of the blade. This fact simplifies substantially the measurement uncertainty analysis,

because the uncertainty associated with the measurement only correspond to the pressure modulus and phase uncertainty of the first harmonic.

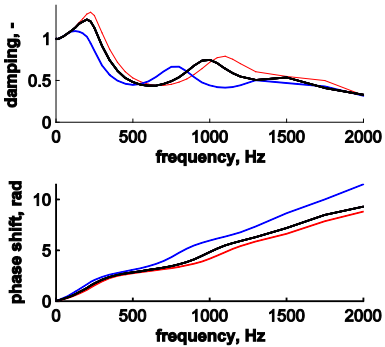
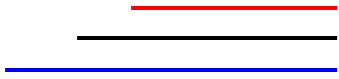
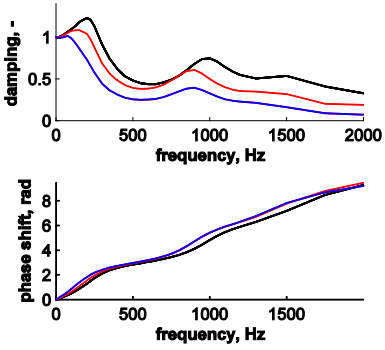
For analyzing how is the reconstruction is affected a 200.2Hz signal obtained with the pressure pulse generator has been analyzed. The unsteady pressure measured by the transducer has been decomposed into the frequency domain and applying the correction procedure has been obtained the estimated pressure in the tap and phase corresponding to the first harmonic. The same procedure has been done with the reference transducer situated in the reference cavity. The result shown in figure() shows a good agreement of the signals (reference and estimated) and the uncertainty window of the measurement, that in this specific case shows an uncertainty in pressure modulus of 4% and a phase uncertainty of 0.01rad. This represented by the curves in blue and green that show the maximum and min amplitude and max and min phase, defining in this way the uncertainty enclosure.

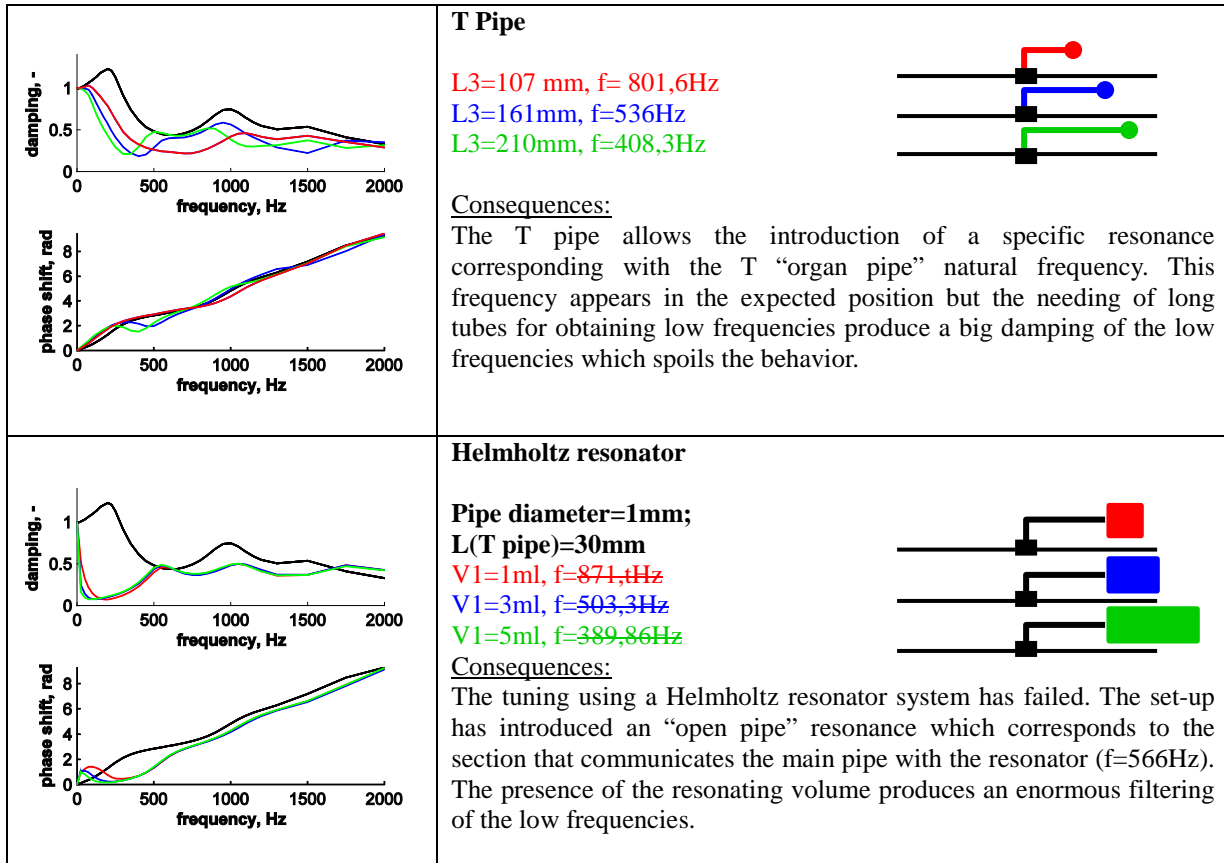
The natural continuation of this work will be the analysis of how is this uncertainty transmitted onto the unsteady blade loading, the subsequently will allow the determination of the aerodynamic damping of the system.

In consequence the modulus and phase uncertainty at can be directly applied into an unsteady blade loading, this will provide the blade unsteady loading uncertainty enclosure that after an integration the imaginary force obtained will provide de aerodynamic damping and its uncertainty.

SYSTEM TUNING PROCEDURES OVERVIEW

The calibrating set up resonances have shown up to be interesting for measuring the unsteady pressure in recessed mounted transducers. At this point the question is if using different piping systems can be tuned the system for introducing the resonance at specific positions. With this purpose different experiments have been done:

	<p>Pipe length</p> <p>L1=48mm L1=68mm (baseline) L1=118m</p>  <p><u>Consequences:</u> A pipe length reduction, increase the main resonance frequency which leads to a mayor influence of the resonance. The phase lag is smaller as well, so in conclusion this is an interesting way for increasing the resonances.</p>
	<p>Pipe section increase</p> <p>L2=10mm L2=30mm</p>  <p><u>Consequences:</u> The introduction of a section increase module produces a reduction of the resonance reducing the appearance frequency, so the overall behavior is spoiled due to the big damping of the signal produced.</p>



CONCLUSIONS

The present paper has analyzed the key aspects which are influenced by a resonance in the calibration set up as well as the possible techniques for resonance manipulation.

The recessed-mounted transducer system and the calibration procedure have shown a big robustness from the point of view of uncertainty assessment and detection of possible uncertainty sources. The capability of detecting the uncertainty sources allows the error tracing along the processing chain providing a good overview of how do each source is affected by the resonances in the calibration.

The results show up interesting reduction of the overall relative uncertainty of the damping determination with respect to the trend (in the frequency band of interest, and in higher frequency resonances) which is translated into an uncertainty reduction of the unsteady pressure estimation. The sources of error analyzed, in this case have revealed a different behavior from the uncertainty point of view. On the one hand, the systematic uncertainty is reduced due to the resonance because the amplification of the signal is bigger than the amplification of the uncertainty. On the other hand the positioning uncertainty that is physically ligated to the duct geometrical properties induces an increase of the uncertainty in the resonant zones due to the change in the resonant properties. At last the random error can be assumed that is not affected by the resonance and its order of magnitude makes it the least significant.

As conclusion, the most significant uncertainty source is the systematic, which only depends on the transducer properties and the analog digital converter and amplification. A good improvement could be to reduce as much as possible the amplification of the signal for increasing the number analog to digital sampling points or to modify acquisition system to be able to set the full resolution of the A/D converter on the unsteady signal. This second improvement is not possible at the present time but is considered to be the best procedure for reducing the uncertainty. It could be also interesting to select the transducers and use the ones with the smallest steady calibration factor (Eq. 3). This will reduce significantly the uncertainty associated with the “measurement steady correction”.

The uncertainty of the estimated pressure will depend directly on the uncertainty of the reference transducer pressure. This fact has shown up as the leading factor for the high frequencies uncertainty. Being the damping uncertainty the most influential for the low frequencies and especially the systematic. The phase lag shows a similar behavior.

For analyzing the unsteady pressures on the blade surface produced by a blade controlled oscillation, only the first harmonic is needed. This fact indicates that the unsteady loading uncertainty is only subjected to the uncertainty associated with the first harmonic of the unsteady pressure.

For other applications in which a mayor number of harmonics are needed to be taken into account, the uncertainty of the measurement will be subjected to the number of harmonics. As the wave reconstruction is based on the assembly of sinusoidal signals at the frequencies indicated by each harmonic and with the corresponding phase, the uncertainty of each harmonic will contribute to the final measurement uncertainty. This fact is needed to be taken into account for determining which harmonics keeps the uncertainty into acceptable limits providing a good agreement with the original signal.

In the end different tuning procedures have been used for adjusting the damping resonances. Among the different test the only one with interesting application is the reduction of the piping system length. Unfortunately the length of this pipe is limited by the physical set up; the blade length, the connector, and the needing of a smooth transition between the stainless steel pipe and the connector. All the rest of the procedures introduce a big fluid volume to the system and increase the internal surface extension, which ultimately spoils damping response at low frequencies. As a final remark the usage of the set up so called Helmholtz, provides a low frequency signal filter that can be used in other applications.

REFERENCES

A Technique For Using Recesed-Mounted Pressure Transducers To Measure Unsteady Pressure.
Vogt, D. M., Fransson, T. H., 2004

Measurement techniques for unsteady flows in turbomachines
C. H. Sieverding, T. Arts, R. DeÂnos, J.-F. Brouckaert, 2000

Measurement Systems, application and design
Ernest O. Doebelin, ISBN 0-07-017336-2

Describing the Uncertainties in Experimental Results
Robert J. Moffat, 1988

HANDBOOK. UNCERTAINTY IN GAS TURBINE MEASUREMENTS
Dr. R. B. Abernethy, Pratt & Whitney ,J. W. Thompson, Jr., 1973